Hindawi Publishing Corporation
Journal of Combustion
Volume 2012, Article ID 927081, 8 pages
doi:10.1155/2012/927081

Research Article

Extending Lean Operating Limit and Reducing Emissions of Methane Spark-Ignited Engines Using a Microwave-Assisted Spark Plug

Vi H. Rapp,[1] Anthony DeFilippo,[1] Samveg Saxena,[1] Jyh-Yuan Chen,[1] Robert W. Dibble,[1] Atsushi Nishiyama,[2] Ahsa Moon,[2] and Yuji Ikeda[2]

[1] *Department of Mechanical Engineering, University of California, Berkeley, 50B Hesse Hall, Berkeley, CA 94720-1740, USA*
[2] *Imagineering Inc., Room 351, Welv Rokko 2nd Building, 4-1-1 Fukada, Nada, Kobe 657-0038, Japan*

Correspondence should be addressed to Vi H. Rapp, vhrapp@berkeley.edu

Received 10 May 2012; Accepted 4 July 2012

Academic Editor: ShiYong Liao

A microwave-assisted spark plug was used to extend the lean operating limit (lean limit) and reduce emissions of an engine burning methane-air. In-cylinder pressure data were collected at normalized air-fuel ratios of $\lambda = 1.46$, $\lambda = 1.51$, $\lambda = 1.57$, $\lambda = 1.68$, and $\lambda = 1.75$. For each λ, microwave energy (power supplied to the magnetron per engine cycle) was varied from 0 mJ (spark discharge alone) to 1600 mJ. At lean conditions, the results showed adding microwave energy to a standard spark plug discharge increased the number of complete combustion cycles, improving engine stability as compared to spark-only operation. Addition of microwave energy also increased the indicated thermal efficiency by 4% at $\lambda = 1.68$. At $\lambda = 1.75$, the spark discharge alone was unable to consistently ignite the air-fuel mixture, resulting in frequent misfires. Although microwave energy produced more consistent ignition than spark discharge alone at $\lambda = 1.75$, 59% of the cycles only partially burned. Overall, the microwave-assisted spark plug increased engine performance under lean operating conditions ($\lambda = 1.68$) but did not affect operation at conditions closer to stoichiometric.

1. Introduction

Concerns with greenhouse gases, air quality, and shortage of fossil fuels have encouraged the development of new technology and alternative fuels that reduce emissions of combustion engines. Natural gas (containing mostly methane) offers lower greenhouse gas emissions than other hydrocarbon fuels because of its high hydrogen-to-carbon ratio. Natural gas can also be combusted at high compression ratios without the risk of producing engine knock. Burning natural gas (containing mostly methane) with air-fuel ratios larger than stoichiometric (lean conditions) in spark-ignited engines has the potential to produce lower emissions and higher thermal efficiencies than petroleum-burning engines [1, 2]. However, if the air-fuel mixture is too lean, the high amount of air dilution destabilizes combustion, decreasing flame speeds and making the air-fuel mixture more difficult to ignite [3, 4]. When combustion becomes unstable due to increased air dilution, engine performance and efficiency deteriorate, limiting the full potential of lean combustion. This unstable combustion point is well known as the "lean limit."

One method of increasing burn rates of lean natural gas mixtures and extending the lean limit is to increase turbulent mixing inside the combustion chamber. Das and Watson [1] modified an engine to increase turbulent mixing by swirling the charge during induction and using a squish motion during the compression stroke, which broke up the intake-generated turbulence into small-scale turbulence inside the combustion chamber. Using this technique and changing the compression ratio, Das and Watson were able to operate the engine at normalized air-fuel ratio (λ) of 1.88. However, the peak thermal efficiency occurred at $\lambda = 1.20$. The engine also produced less carbon dioxide (CO_2), hydrocarbon, and nitrogen oxide (NO_x) emissions than equivalent petroleum engines. Evans [5] achieved similar results using a "squish-jet" combustion chamber but also investigated the effects of

a partially stratified-charge mixture near the spark plug to enhance ignition of lean mixtures. Evans' results showed that the partially stratified-charge combustion system extended the lean limit of operation and reduced NO_x emissions. Cho and He [6] found that delaying fuel injection reduced CO and HC emissions at 25% throttle and 100% throttle.

Another method for stabilizing lean operation and reducing emissions is addition of hydrogen to natural gas-fueled engines. Several researchers have shown that addition of hydrogen increases flame propagation of the air-fuel mixture, extending the lean operating limit and reducing emissions [7–14]. Smutzer [8] developed a hydrogen-assisted lean operation (HALO) engine that achieved operation at ultralean conditions ($\lambda = 2.0$), eliminating NO_x production and reduced spark ignition energy by 22%. However, nonuniformities in fueling lead to high cylinder-to-cylinder variation in the engine. Wang et al. [10] investigated the cycle-to-cycle variations in natural gas-hydrogen blends and found that addition of hydrogen is strongly correlated with peak in-cylinder pressure, pressure rise rate, and crank angle degree of peak in-cylinder pressure. They also found that addition of hydrogen decreased cycle-to-cycle variation under stoichiometric conditions and lean conditions. Kornbluth et al. [11] found that adding hydrogen (30%–50% by volume) to landfill gas (containing mostly methane and CO_2) while operating under lean conditions increased engine stability and power, while decreasing emissions, especially NO_x. Their results also show that increasing the concentration of hydrogen extended the lean limit [11].

High-energy ignition devices have also been used to extend lean limits beyond the capabilities of a traditional spark discharge ignition systems [15, 16]. One such high-energy ignition technology of current research interest is the microwave-assisted spark plug, under development by Imagineering Inc., which delivers microwaves into the combustion chamber in addition to the standard spark discharge [17, 18]. A capacitive discharge spark initiates plasma in the combustion chamber, and microwaves expand the plasma. As compared to arc discharges, which traditionally ignite internal combustion engines, microwave plasma discharges are characterized by higher spatial uniformity, lower plasma potential, higher electron energy, and increased excitation of vibrationally and electronically excited states of molecules [19]. High-energy electrons, having received energy from microwaves, can enhance mixture reactivity through electron impact reactions which generate radicals and metastable electronically excited chemical species [19]. Past studies have shown that a microwave-assisted spark plug can extend the lean limit of gasoline-fueled engines [17, 20, 21] and that microwaves can enhance flame speed in wall-stagnated methane flames [22].

Although the microwave-assisted spark plug has proven effective for gasoline-fueled engines operating under lean conditions [17, 20, 21], its effectiveness has not previously been demonstrated for use on engines burning methane-based fuels (such as natural gas). For this study, a single-cylinder engine burning methane-air was modified to operate using a microwave-assisted spark plug system. The performance of the microwave-assisted spark discharge was compared to the spark-only discharge over a range of air-fuel ratios and microwave energy levels.

Following this section, the instrumentation, experimental design, and variables used to measure engine stability and performance are described. Next, results and discussions are presented. Last, conclusions are made, and future work is suggested.

Table 1: Engine specifications.

Displacement	0.616 L
Stroke	114.3 mm
Bore	82.8 mm
Connecting rod	254 mm
Number of valves	2
IVO at 0.15 mm lift	$-343°$CA ATDC$_{compression}$
IVC at 0.15 mm lift	$-153°$CA ATDC$_{compression}$
EVO at 0.15 mm lift	$148°$CA ATDC$_{compression}$
EVC at 0.15 mm lift	$-353°$CA ATDC$_{compression}$

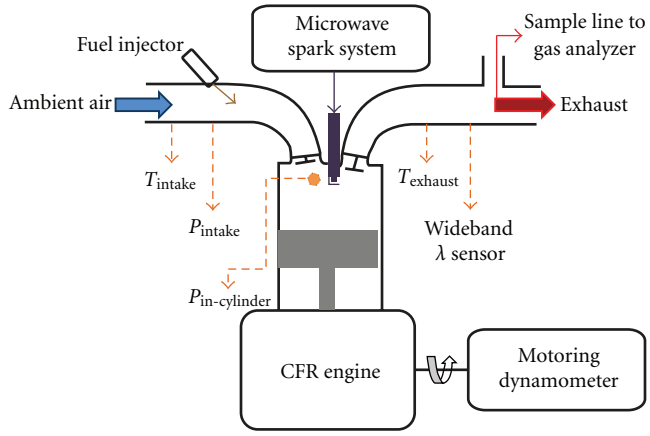

Figure 1: Schematic of Cooperative Fuel Research (CFR) engine with microwave-assisted spark plug system. Sensors are marked with dashed lines.

2. Material and Methods

2.1. Engine Specifications. Experiments were conducted using a single cylinder Waukesha ASTM-Cooperative Fuel Research (CFR) engine. Engine specifications can be found in Table 1. A schematic of the CFR engine with the microwave-assisted spark plug system is shown in Figure 1. A compressed gas cylinder supplied methane to the CFR gaseous fuel injector. The CFR engine was fitted with the Imagineering, Inc. microwave-assisted spark plug system, which transmits 2.45 GHz microwaves into the combustion chamber through the spark plug insulator. The microwaves interact with plasma initiated by a 30 mJ capacitive spark discharge [17].

2.2. Measurement Instrumentation. In-cylinder pressure was measured using a 6052B Kistler piezoelectric pressure transducer in conjunction with a 5044A Kistler charge amplifier

Table 2: Engine operating conditions.

Compression ratio	10 : 1
Engine speed	1200 RPM
Coolant temperature	75.0 ± 1.00°C
Intake pressure	100.0 ± 0.5 kPa
Intake temperature	28.0 ± 1°C
Fuel	Methane
Throttle position	100%

and was recorded every 0.1 crank angle (CA) degree. The cylinder pressure transducer was mounted in the cylinder head. Intake pressure was measured using a 4045A5 Kistler piezoresistive pressure transducer in conjunction with a 4643 Kistler amplifier module. Intake temperature and exhaust temperature were measured using K-type thermocouples. Crank angle position was determined using an optical encoder, while an electric motor, controlled by an ABB variable speed frequency drive, controlled the engine speed. A Motec M4 ECU (Engine Control Unit) controlled injection timing, injection pulse width, and injection duty cycle. A Horiba analyzer measured emissions and equivalence ratio. A wideband lambda sensor was used to establish stoichiometric conditions and compared with emissions results. Figure 1 shows a schematic of the engine with the location of each sensor.

2.3. Experimental Design. Microwave-assisted spark plug performance was explored over a range of microwave energy inputs, normalized air-fuel ratios (λ), and spark timings. Compression ratio and engine speed were held constant, and the engine was operated naturally aspirated at wide-open throttle. Engine operating conditions are outlined in Table 2. At each operating condition, spark timing was adjusted to achieve Maximum Brake Torque (MBT), at which point 300 thermodynamic cycles of in-cylinder pressure data were recorded (each cycle consisting of 720 CAD). The parameter space of normalized air-fuel ratio included $\lambda = 1.46$, $\lambda = 1.51$, $\lambda = 1.57$, and $\lambda = 1.75$. The parameter space of total energy supplied to the magnetron per engine cycle included 0 mJ (spark only), 130 mJ, 900 mJ, and 1600 mJ. The 130 mJ energy input condition was achieved by supplying the magnetron with peak power of 2.6 kW at a 12.5% duty cycle over a 0.36 ms duration. The 900 mJ and 1600 mJ conditions also operated with peak input power of 2.6 kW, but with 25% duty cycle and durations of 1.32 ms and 2.65 ms, respectively. The power supplied to the magnetron falls off with increasing duration, explaining why total energy input does not scale linearly with energy input duration. The total microwave energy delivered to the combustion chamber is estimated to be approximately 17% of the energy supplied to the magnetron after accounting for reflection and transmission losses.

2.4. Data Analysis. The performance of the microwave-assisted spark plug is characterized by using the indicated mean effective pressure (IMEP) and the indicated thermal efficiency [23]. Engine stability is characterized by two parameters. The first parameter is the coefficient of variation of the IMEP (COV_{IMEP}):

$$\text{COV}_{\text{IMEP}} = \frac{\sigma_{\text{IMEP}}}{x_{\text{IMEP}}} \times 100, \quad (1)$$

where σ_{IMEP} is the standard deviation in IMEP and x_{IMEP} is the mean IMEP [23]. COV_{IMEP} increases when engine operation becomes unstable, leading to partial burn cycles and misfires [23].

The second parameter is the modified pressure ratio (MPR):

$$\text{MPR} = \frac{p_{\max}}{p_{\text{motoring-max}}} - 1, \quad (2)$$

where $p_{\max}$ is the maximum pressure with ignition and $p_{\text{motoring-max}}$ is the maximum pressure while motoring (no ignition) [24]. The MPR determines if a cycle has completely combusted, partially burned, or misfired (no combustion) [24]. For methane, at $\lambda = 1.68$, the limits of complete combustion, partial burn, and misfire were identified as

$$\text{complete } 1.8 < \text{MPR} \leq 3.5,$$
$$\text{partial burn } 0.5 < \text{MPR} \leq 1.8,$$
$$\text{misfire } 0 \leq \text{MPR} \leq 0.5.$$

Under lean conditions, the normalized air-fuel ratio, λ, was calculated using

$$\lambda = \frac{m_{f,\text{stoich}}}{m_f}, \quad (3)$$

where $m_{f,\text{stoich}}$ is the stoichiometric mass of the fuel injected per cycle and m_f is the actual mass of the fuel injected per cycle [23, 25].

The change in emissions is determined by

$$\%\ \text{change in emissions} = \left(\frac{\text{ppm}_{\text{MW}}}{\text{ppm}_{\text{Spk}}} - 1\right) \times 100, \quad (4)$$

where ppm_{MW} is the measured emission in ppm when microwave energy is added and ppm_{Spk} is the measured emissions in ppm when no microwave energy is added (spark only).

Uncertainty in measured data is reported as mean ± uncertainty with a confidence level of 95%. Uncertainty in calculated parameters is reported from an uncertainty analysis, and the details can be found in the Appendix.

3. Results and Discussion

The performance of the microwave-assisted spark plug is gauged by the following: engine stability, engine power, and emissions output. Engine stability is expressed by COV_{IMEP} and the percentage of complete combustion cycles. Engine power and performance are given by IMEP and the indicated thermal efficiency. Emissions output for each experiment is provided and compared with stability and performance variables.

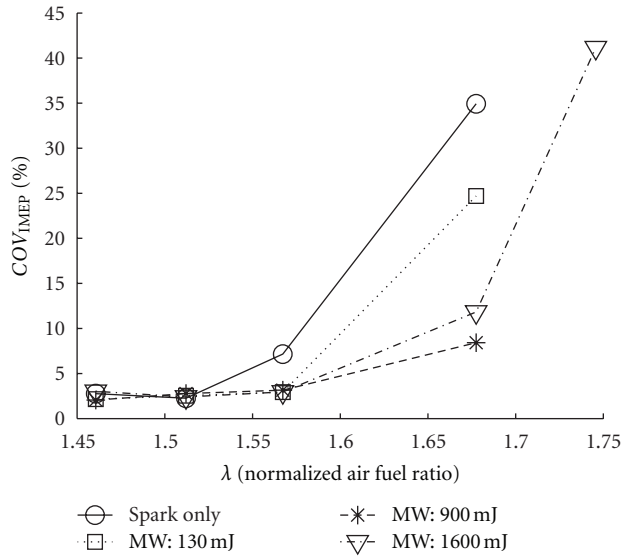

Figure 2: Engine stability increases with the addition of microwave energy as λ increases. Increasing microwave energy from 900 mJ to 1600 mJ did not further increase engine stability.

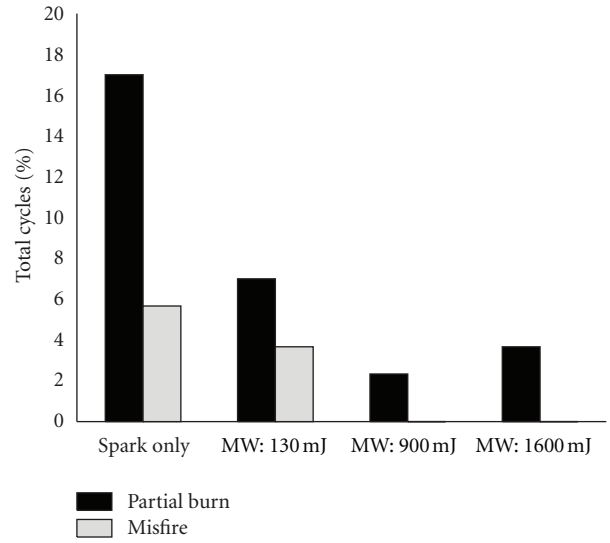

Figure 3: At $\lambda = 1.68$, adding microwave energy to the spark discharge per cycle decreases occurrence of misfire and partial-burn cycles, thus increasing the total number of complete combustion cycles.

3.1. Engine Stability. Engine operation was considered to be stable when COV_{IMEP} was no more than 10%, and the percentage of complete combustion cycles was at least 95%. Shown in Figure 2 is the dependence of COV_{IMEP} on λ for all operating conditions. At the leanest operating condition ($\lambda = 1.75$), stable combustion could not be achieved, and multiple misfires occurred using a standard spark discharge. Supplying 1600 mJ per engine cycle to the magnetron consistently ignites the mixture, shown in Figure 2; however, the COV_{IMEP} is 41%, and the percentage of complete combustion cycles is 37% (59% partial burn and 4% misfire), indicating unstable operation.

Decreasing λ to 1.68 continued to result in unstable operation when using a standard spark discharge. Figure 2 shows the COV_{IMEP} is 35% and the percentage of complete combustion cycles is 77%, while 17% of the cycles partially burn and 6% of the cycles misfire as seen in Figure 3. Adding 130 mJ of energy to the microwave system decreases COV_{IMEP} to 25% and increases the number of complete combustion cycles to 89% (7% partial burn cycles and 4% misfire). Further addition of microwave energy (900 mJ) decreases COV_{IMEP} to 8% and increases the complete combustion cycles to 98% (2% partial burn cycles), resulting in stable operation. Figure 2 shows that addition of 1600 mJ of microwave energy decreases engine stability; however, the difference in partial burn cycles and thermal efficiency from the 900 mJ case was less than 2% for both. The observed small difference implies that adding 1600 mJ of energy neither decreases nor further improves engine stability. These results also suggest that the microwave input may be most effective during the earliest stage of ignition since the 1600 mJ and the 900 mJ energy inputs have the same power, but the 1600 mJ setting is operated for a longer duration, as stated in the methods. Addition of microwave energy did not affect COV_{IMEP} at operating conditions closer to stoichiometric ($\lambda < 1.52$) because almost all the cycles (>99%) completely burned.

3.2. Engine Power and Performance. Engine power and performance are given by IMEP and the indicated thermal efficiency. Figure 4 shows IMEP decreases with increasing λ for all operating conditions. For $\lambda > 1.55$, the microwave-assisted spark plug increases engine performance by enhancing burning, leading to better engine stability. At $\lambda = 1.68$, addition of microwave energy slightly increases IMEP. For $\lambda < 1.55$, the microwave appears to have almost no effect on IMEP.

For the standard spark discharge, Figure 5 shows an increase in indicated thermal efficiency as air-fuel ratio increases from $\lambda = 1$ to $\lambda = 1.46$. Beyond $\lambda = 1.46$, the indicated thermal efficiency decreases due to incomplete combustion. Addition of microwave energy at $\lambda = 1.68$ increases indicated thermal efficiency by up to 4% but shows minimal improvement between $\lambda = 1.46$ and $\lambda = 1.57$. The peak indicated thermal efficiency occurred at $\lambda = 1.46$, which are slightly leaner conditions than previous studies burning only natural gas [1, 6].

3.3. Engine Emissions. The effects of the microwave spark-plug system on emissions were explored by normalizing the microwave operating condition emissions with the standard spark discharge emissions and finding the percent difference (see (4)). Figure 6 shows NO_x production increases when the engine is run with 1600 mJ of microwave energy. At $\lambda = 1.46$, when stable combustion is unaffected by microwaves, microwave-enhanced ignition increases NO_x production by 13% (about 100 ppm), indicating a small direct contribution of the added microwave energy towards NO_x formation. As

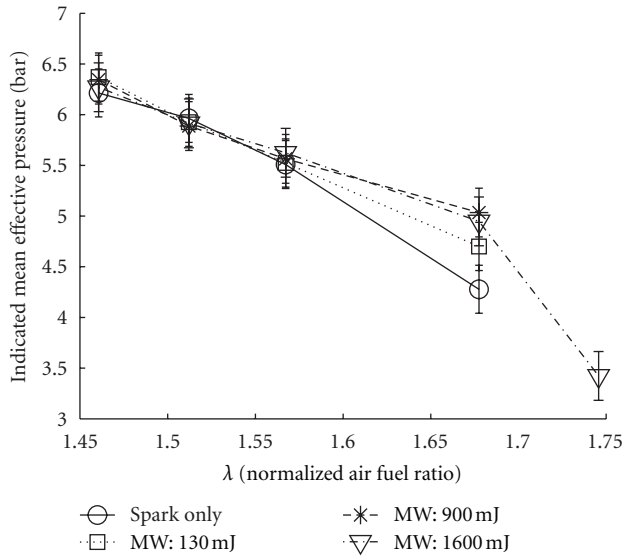

Figure 4: Addition of microwave energy slightly increased IMEP at larger λ. Increasing microwave energy did not further increase IMEP. Error bars are ± the uncertainty calculated using propagation of error (see Appendix A).

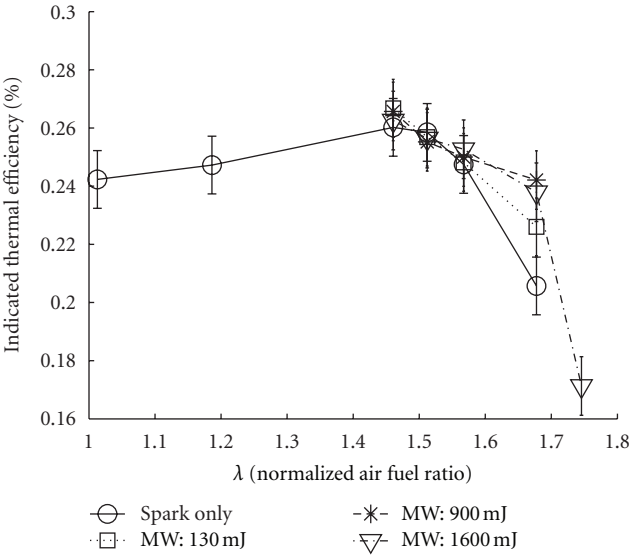

Figure 5: Addition of microwave energy increases thermal efficiency at $\lambda = 1.68$. Error bars are ± the uncertainty calculated using propagation of error (see Appendix A).

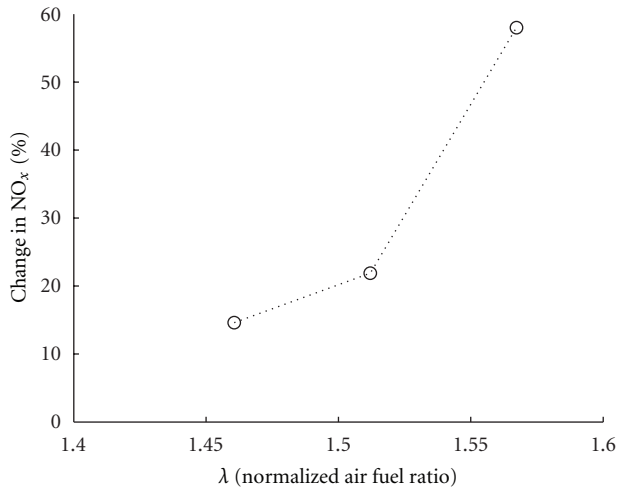

Figure 6: The percent change in NO_x emissions with 1600 mJ microwave-enhanced ignition from NO_x emissions with spark-only ignition. Under stable operating conditions ($\lambda = 1.46$), addition of microwave energy increases NO_x production by 13% (~100 ppm). Increasing λ further increases NO_x.

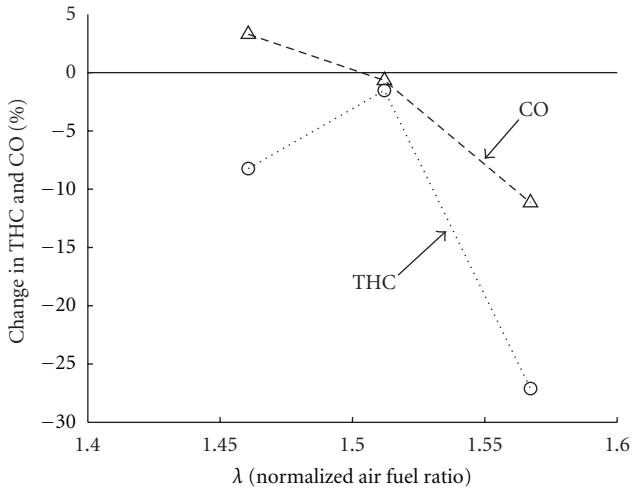

Figure 7: The percent change in carbon-monoxide (CO) emissions and total unburned hydrocarbon (THC) emissions with 1600 mJ of microwave-enhanced ignition from emissions with spark-only ignition. Addition of microwave energy decreases the amount of CO and THC at leaner conditions. A decrease in THC is expected under lean operation with the microwave because more cycles are complete combustion.

operating conditions become leaner ($\lambda = 1.57$ and $\lambda = 1.68$,) the difference in NO_x production between spark-only and microwave-enhanced operation widens. This increase is due to an increase in complete combustion cycles when the engine is operating with microwave energy in addition to the direct contribution of NO_x when adding microwave energy. The minimum NO_x measurement for all operating conditions was 3.75 g/kWh.

Figure 7 shows that addition of 1600 mJ of microwave energy decreases carbon monoxide (CO) and total unburned hydrocarbons (THC) as operating conditions become leaner. This trend agrees with previous results [11] and is due to an increase in complete combustion cycles with the addition of microwave energy under leaner operating conditions ($\lambda > 1.51$).

4. Conclusions and Recommendations

In this study, we found that a microwave-assisted spark plug extends the lean stable operating limit of an engine

burning methane-air. The addition of microwave energy improved engine stability and as a result also increased engine performance. At the leanest operating condition ($\lambda = 1.75$), a standard spark discharge did not consistently ignite the air-fuel mixture and resulted in multiple misfires. However, with the addition of microwave energy, the mixture ignited, resulting in mostly partial burn cycles (59%) and few misfire cycles (4%). Decreasing the normalized air-fuel ratio from $\lambda = 1.75$ to $\lambda = 1.68$ allowed for engine performance comparisons between the spark discharge alone and the spark discharge with microwave energy assistance. Addition of microwave energy at $\lambda = 1.68$ increased the number of complete combustion cycles, the indicated mean effective pressure, and the indicated thermal efficiency.

Increasing the total microwave energy input to the magnetron per cycle from 130 mJ to 900 mJ improved engine stability. Further increasing input energy to the microwave system from 900 mJ to 1600 mJ by increasing the duration of energy input showed no additional improvements. These results suggest that microwave input may be effective only during the earliest stage of ignition, when a small flame kernel is still present near the spark plug electrode. For richer mixtures ($\lambda < 1.52$), microwave energy did not improve engine stability because almost all the cycles completely burned.

Addition of microwave energy decreased CO and total unburned hydrocarbon emissions but increased NO_x emissions. The increase in NO_x is due to an increase in complete combustion cycles when microwave energy is added to the ignition. Also, under leaner operating conditions ($\lambda = 1.57$), combustion advances slightly, allowing more time for NO_x formation.

The present microwave-assisted spark plug fully eliminated misfires under lean conditions ($\lambda = 1.68$) and could likely allow for steady, lean operation when burning other alternative fuels. However, performance of the microwave-assisted spark plug should be further tested using alternative fuels. Using a higher-turbulence engine with the microwave spark-plug system may also increase power output and further extend the lean limit. Additionally, investigating flame occurrence and propagation using optical techniques may also provide further insight on the effectiveness of a microwave-assisted spark plug.

Appendix

A. Uncertainty Analysis

An uncertainty analysis was performed on all engine measurements and calculations, except emissions. For the measured values, the random uncertainty was calculated using 95% confidence intervals (approximately 2 times the standard error, $\sigma_{\bar{x}}$ for normally distributed errors) [26]:

$$R_x = 2 \times \sigma_{\bar{x}} = \frac{2\sigma_x}{\sqrt{N}}, \tag{A.1}$$

where x is the measured value, N is the number of cycles, σ_x is the standard deviation, defined as

$$\sigma_x = \left(\frac{1}{N-1} \sum_{i=1}^{N} (x_i - \bar{x})^2 \right)^{1/2}, \tag{A.2}$$

and $\bar{x}$ is the mean of the measured values.

The general formula for error propagation in an equation with multiple variables was calculated using [26, 27]

$$U_r = \sqrt{\left(\frac{\partial r}{\partial x_1} U_{x_1} \right)^2 + \left(\frac{\partial r}{\partial x_2} U_{x_2} \right)^2 + \cdots + \left(\frac{\partial r}{\partial x_n} U_{x_n} \right)^2}, \tag{A.3}$$

where uncertainty is being measured in r and x_n are independent variables with measured uncertainties. This error propagation formula was used to determine the uncertainty in calculated variables.

A.1. In-Cylinder Pressure. As mentioned previously, the in-cylinder pressure was measured using a 6052B Kistler piezoelectric pressure transducer in conjunction with a 5044A Kistler charge amplifier. The systematic error for the transducer, B_P, is listed as 0.2 bar. Random uncertainty in the pressure data was calculated using (A.1) and a minimum of 300 cycles.

Using the random uncertainty and the systematic error in the pressure, the total uncertainty in pressure can be calculated using [26, 27]

$$U_p = \sqrt{R_p^2 + B_p^2}. \tag{A.4}$$

A.2. Volume. The volume at each crank angle degree can be calculated by [27]

$$V = V_c + \frac{\pi B^2}{4} \left(l + a - a\cos\theta - \left(l^2 - a^2 \sin^2\theta \right)^{1/2} \right), \tag{A.5}$$

where V_C is the clearance volume, B is the bore, l is the connecting rod length, and a is crank radius [23]. Top Dead Center (TDC) of the motoring traces was calculated using the method outlined by Tunestal [28]. The uncertainty in crank angle degree, using Tunestal's method to find TDC, is 0.05°. The uncertainty in volume can be determined using

$$U_V = \frac{dV}{d\theta} U_\theta, \tag{A.6}$$

where

$$\frac{dV}{d\theta} = \frac{1}{4} \pi B^2 \left(a \sin\theta + \frac{a^2 \sin\theta \cos\theta}{\sqrt{l^2 - a^2 \sin^2\theta}} \right). \tag{A.7}$$

A.3. Indicated Work. The indicated work is calculated using the trapezoidal method of integration:

$$W = \sum_{i}^{n-1} \Delta V_i \frac{p_{i+1} + p_i}{2}, \tag{A.8}$$

where n is the number of divisions and p is the pressure [23]. Using (A.3), the uncertainty in the work can be determined by

$$U_W^2 = \left(\frac{\partial W}{\partial \Delta V_1} U_{\Delta V_1}\right)^2 + \left(\frac{\partial W}{\partial p_1} U_{p_1}\right)^2 + \left(\frac{\partial W}{\partial p_2} U_{p_2}\right)^2 + \cdots + \left(\frac{\partial W}{\partial \Delta V_{n-1}} U_{\Delta V_{n-1}}\right)^2 + \left(\frac{\partial W}{\partial p_{n-1}} U_{p_{n-1}}\right)^2 + \left(\frac{\partial W}{\partial p_n} U_{p_n}\right)^2. \tag{A.9}$$

A.4. Indicated Power, IMEP, and Indicated Thermal Efficiency. Knowing the uncertainty in the work, the uncertainty in the indicated power indicated mean effective pressure (IMEP), and the indicated thermal efficiency (η_{th}) can be determined using the equation for uncertainty in products and quotients:

$$\left(\frac{U_r}{|r|}\right)^2 = \left(\frac{U_{x_1}}{|x_1|}\right)^2 + \left(\frac{U_{x_2}}{|x_2|}\right)^2 + \cdots \left(\frac{U_{x_n}}{|x_n|}\right)^2, \tag{A.10}$$

where uncertainty is being measured in r and x_n are independent variables with measured uncertainties [27].

Using (A.10), the uncertainty in indicated power (P_i), IMEP, and η_{th} can be determined by the following:

$$U_{P_i} = P_i\left(\frac{U_W}{W}\right),$$
$$U_{\text{IMEP}} = \text{IMEP}\left(\frac{U_W}{W}\right), \tag{A.11}$$
$$U_{\eta_{\text{th}}} = \eta_{\text{th}}\left(\frac{U_W}{W}\right).$$

Acknowledgments

This research was partially supported by the University of Michigan, Award no. 3001397038, through a cooperative agreement with the US Department of Energy entitled "A University Consortium on High Pressure Lean Combustion (HPLC) for Efficient and Clean ICE." The authors wish to acknowledge the assistance of T. Dillstrom, N. Killingsworth, and M. Wissink in conducting experimental measurements.

References

[1] A. Das and H. C. Watson, "Development of a natural gas spark ignition engine for optimum performance," *Proceedings of the Institution of Mechanical Engineers D*, vol. 211, no. 5, pp. 361–378, 1997.

[2] H. M. Cho and B. Q. He, "Spark ignition natural gas engines—a review," *Energy Conversion and Management*, vol. 48, no. 2, pp. 608–618, 2007.

[3] A. A. Quader, "What limits lean operation in spark ignition engines-flame initiation or propagaion?" SAE Paper 760760, 1976.

[4] H. Li, G. A. Karim, and A. Sohrabi, "The lean mixture operational limits of a spark ignition engine when operated on fuel mixtures," *Journal of Engineering for Gas Turbines and Power*, vol. 131, no. 1, Article ID 012801, 2009.

[5] R. L. Evans, "Extending the lean limit of natural-gas engines," *Journal of Engineering for Gas Turbines and Power*, vol. 131, no. 3, Article ID 032803, 2009.

[6] H. M. Cho and B. Q. He, "Combustion and emission characteristics of a lean burn natural gas engine," *International Journal of Automotive Technology*, vol. 9, no. 4, pp. 415–422, 2008.

[7] P. Tunestal, M. Christensen, P. Einewall, T. Andersson, and B. Johansson, "Hydrogen addition for improved lean burn capability of slow and fast burning natural gas combustion chambers," SAE Paper 2002-01-2686, 2002.

[8] C. Smutzer, *Application of Hydrogen Assisted Lean Operation To Natural Gas-Fueled Reciprocating Engines (HALO)*, TIAX LLC, 2006.

[9] F. Ma and Y. Wang, "Study on the extension of lean operation limit through hydrogen enrichment in a natural gas spark-ignition engine," *International Journal of Hydrogen Energy*, vol. 33, no. 4, pp. 1416–1424, 2008.

[10] J. Wang, H. Chen, B. Liu, and Z. Huang, "Study of cycle-by-cycle variations of a spark ignition engine fueled with natural gas-hydrogen blends," *International Journal of Hydrogen Energy*, vol. 33, no. 18, pp. 4876–4883, 2008.

[11] K. Kornbluth, J. Greenwood, Z. McCaffrey, D. Vernon, and P. Erickson, "Extension of the lean limit through hydrogen enrichment of a LFG-fueled spark-ignition engine and emissions reduction," *International Journal of Hydrogen Energy*, vol. 35, no. 3, pp. 1412–1419, 2010.

[12] K. Nanthagopal, R. Subbarao, T. Elango, P. Baskar, and K. Annamalai, "Hydrogen enriched compressed natural gas—a futuristic fuel for internal combustion engines," *Thermal Science*, vol. 15, pp. 1145–1154, 2011.

[13] S. S. Sandhu, M. K. G. Babu, and L. M. Das, "Investigation of emission characteristics and thermal efficiency in a spark-ignition engine fuelled with natura gas-hydrogen blends," *International Journal of Low-Carbon Technologies*. In press.

[14] W. Xin, Z. Hong-guang, L. Yan et al., "Effects of engine operating parameters on lean combustion limit of hydrogen enhanced natural gas engine," *Anvanced Materials Research*, vol. 383–390, pp. 6116–6121, 2012.

[15] J. D. Dale, M. D. Checkel, and P. R. Smy, "Application of high energy ignition systems to engines," *Progress in Energy and Combustion Science*, vol. 23, no. 5-6, pp. 379–398, 1997.

[16] M. Kettner, A. Nauwerck, U. Spicher, J. Seidel, and K. Linkenheil, "Microwave-based ignition principle for gasoline engines with direct injection and spray guided combustion system," *MTZ Worldwide*, vol. 67, no. 6, pp. 476–480, 2006.

[17] A. DeFilippo, S. Saxena, V. Rapp et al., "Extending the lean stability limits of gasoline using a microwave-assisted spark plug," SAE Paper 2011-01-0663, 2011.

[18] Y. Ikeda, A. Nishiyama, Y. Wachi, and M. Kaneko, "Reseach and development of a microwave plasma combustion engine (Part I: Concept of plasma combustion and plasma generation technique)," SAE Technical Paper 2009-01-1050, 2009.

[19] S. M. Starikovskaia, "Plasma assisted ignition and combustion," *Journal of Physics D*, vol. 39, no. 16, article R265, 2006.

[20] Y. Ikeda, K. Hiroki, M. Jeonj, and H. Kaneko, "Research and development of microwave plasma combustion engine (Part II: Engine performance of plasma combustion engine," SAE Technical Paper 2009-01-1049, 2009.

[21] Y. Ikeda, A. Nishiyama, and M. Kaneko, "Microwave enhanced ignition process for fuel mixture at elevated pressure of 1MPa," in *Proceedings of the 47th AIAA Aerospace Sciences Meeting*

Including the New Horizons Forum and Aerospace Exposition, Orlando, Fla, USA, January 2009.

[22] E. S. Stockman, S. H. Zaidi, R. B. Miles, C. D. Carter, and M. D. Ryan, "Measurements of combustion properties in a microwave enhanced flame," *Combustion and Flame*, vol. 156, no. 7, pp. 1453–1461, 2009.

[23] J. B. Heywood, *Internal Combustion Engine Fundamentals*, McGraw-Hill, 1988.

[24] M. C. Sellnau, F. A. Matekunaus, P. A. Battison, C. F. Chang, and D. R. Lancaster, "Cylinder-pressure-based engine control using pressure-ratio-management and low-cost non-intrusive cylinder pressure sensors," SAE Paper 2000-01-0932, 2000.

[25] R. Stone, *Introduction to Internal Combustion Engines*, MacMillan, London, UK, 1985.

[26] H. W. Coleman and W. G. Steele, *Experimentation, Validation, and Uncertainty Analysis For Engineers*, John Wiley & Sons, 3rd edition, 2009.

[27] J. R. Taylor, *An Introduction To Error Analysis: the Study of Uncertainties in Physical Measurements*, University Science Books, Sausalito, Calif, USA, 2nd edition, 1997.

[28] P. Tunestal, "Model based TDC offset estimation from motored cylinder pressure data," in *Proceedings of the IFAC Workshop on Engine and Powertrain Control, Simulation, and Modeling*, 2009.